Journal of Zhejiang University SCIENCE A
ISSN 1009-3095 (Print); ISSN 1862-1775 (Online)
www.zju.edu.cn/jzus; www.springerlink.com
E-mail: jzus@zju.edu.cn

Galerkin method study on flow of Oldroyd-B fluids in curved circular cross-section pipes*

ZHANG Ming-kan†, SHEN Xin-rong, MA Jian-feng, ZHANG Ben-zhao
(*Institute of Fluid Engineering, Zhejiang University, Hangzhou 310027, China*)
†E-mail: wangtwo@zju.edu.cn
Received Dec. 10, 2005; revision accepted Feb. 26, 2006

Abstract: A Galerkin method was used to investigate steady, fully developed flow of Oldroyd-B fluids through curved pipes of circle cross-section. By using Galerkin method, large values of curvature ratio, Reynolds number and Weissenberg number can be discussed. The powers of the series of the Galerkin method in the present work are chosen carefully. Both effects of Reynolds number and Weissenberg number on axial velocity and stream function are discussed even for large values of the two non-dimensional parameters. It was discovered that the combined effect of large Reynolds number and Weissenberg number decreases the outward shifts of maximum axial velocity and maximum stream function. Axial normal stress of creeping flow is also studied here. The large Weissenberg number makes the stress concentration occur on the inner bend of the pipe.

Key words: Curved pipe, Galerkin method, Oldroyd-B fluid, Flow characteristic, Axial normal stress
doi:10.1631/jzus.2006.AS0263 **Document code:** A **CLC number:** O373

INTRODUCTION

In this study, we obtained the Galerkin solution for steady, fully developed flow of viscoelastic fluids through curved pipes of circular cross-section. Galerkin technique yielding high-order semi-analytical solutions will provide valuable tests for numerical simulations of viscoelastic flows without the small parameters limit of perturbation technique. In addition, it is suitable for examining the coupled effects of viscous, centrifugal and elastic forces on the flow of viscoelastic fluids through curved pipes.

The motion of the steady, fully developed flow in curved pipes has been studied extensively for the case of Newtonian fluids due to its practical importance in various industrial applications. The first analytical solution for such flows was obtained by Dean (1927; 1928) using perturbation technique. He was the first one who found the theoretical existence of cross-section secondary flow. To recognize the importance of centripetal force, in his studies, Dean simplified the equations of motion by ignoring all terms arising due to the pipe curvature except the centripetal force terms. Topakoglu (1967) later extended Dean's work to the full equations of flow for pipes of both circular and annular cross-sections. From then on, many researchers have joined hands to study such flows using both analytical methods and numerical methods. Ito (1969) obtained solutions by using boundary layer method, which could deal with the large Dean number problem. Nandakumar and Masliyah (1982) presented some finite difference solutions for curvature ratio κ as large as 0.1, while Soh and Berger (1987) solved the full N-S equations from κ=0.01 to κ=0.2 using a finite different method. More recently, Zhang *et al*.(2000), Zhang and Zhang (2003) and Chen *et al*.(2003) systemically investigated flow and heat transfer in various types of pipes.

For the case of viscoelastic fluids flow, it is quite surprising to find that, despite its important applications such as food and pharmaceutic products, oil transportation and blood flow, much less attention has been paid to such flow in curved pipes by the mono-

* Project (No. 10272096) supported by the National Natural Science Foundation of China

graphers than its Newtonian counterpart. Using the simplifications introduced by Dean, the flow of viscoelastic fluids in curved pipes of circular cross-section has been examined for the Bingham fluid (Clegg and Power, 1963; Das, 1992), the Reiner-Rivlin fluid (Jones, 1960), the second order fluid (Sharma and Prakash, 1977) and the Oldroyd-B fluid (Thomas and Walters, 1963). Bowen *et al*.(1991) later solved the UCM constitutive equations for the creeping flow without invoking Dean's approximation. More recently, Robertson and Muller (1996) and Jitchote and Robertson (2000) presented perturbation solutions for Oldroyd-B fluid and second order fluid, respectively. Almost at the same time, Fan *et al*.(2001) investigated the comparison between fully developed viscous and viscoelastic flows in curved pipes by using finite element method. In their work, they investigated not only the flow characteristic but the two normal stress differences as well.

This paper is aimed at obtaining analytical solutions of Galerkin method for Oldroyd-B fluids and exploring the secondary flow structures, the axial flow and the axial normal stress distribution of such flow in curved pipes. The governing equations in toroidal coordinate system are obtained by using the tensor analysis from many references to Bolinder (1996)'s work.

GOVERNING EQUATIONS

Fig.1 shows a curved pipe of circular cross-section and the toroidal coordinate system used in the present work. The coordinates are $\tilde{x}$, $\tilde{y}$, $\tilde{s}$, where $\tilde{s}$ is the centerline of the pipe. R and a are the radius of the curved pipe and the radius of the circular cross-section, respectively. The velocities in the directions of $\tilde{x}$, $\tilde{y}$, $\tilde{s}$ are denoted by $\tilde{u}$, $\tilde{v}$, $\tilde{w}$, respectively. Fig.1 also shows the orthonormal basis ($\boldsymbol{e}_x$, $\boldsymbol{e}_y$, $\boldsymbol{e}_s$) defined relative to the rectangular Cartesian basis ($\boldsymbol{e}_1$, $\boldsymbol{e}_2$, $\boldsymbol{e}_3$) as

$$\begin{aligned}\boldsymbol{e}_x &= \cos(\tilde{s}/R)\boldsymbol{e}_1 + \sin(\tilde{s}/R)\boldsymbol{e}_2,\quad \boldsymbol{e}_y = \boldsymbol{e}_3,\\ \boldsymbol{e}_s &= -\sin(\tilde{s}/R)\boldsymbol{e}_1 + \cos(\tilde{s}/R)\boldsymbol{e}_2.\end{aligned} \tag{1}$$

In the constitutive equation of Oldroyd-B fluids, the extra stress tensor $\tilde{\boldsymbol{\tau}}$ can be written as

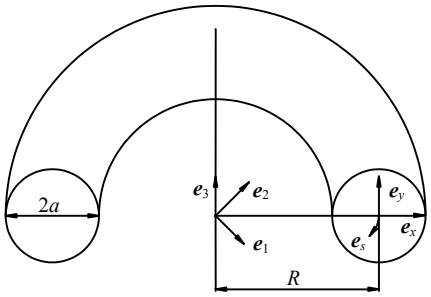

Fig.1 The curved pipe and the coordinate system

$$\tilde{\boldsymbol{\tau}} = \tilde{\boldsymbol{\tau}}^{\mathrm{s}} + \tilde{\boldsymbol{\tau}}^{\mathrm{p}}, \tag{2}$$

where $\tilde{\boldsymbol{\tau}}^{\mathrm{s}}$ and $\tilde{\boldsymbol{\tau}}^{\mathrm{p}}$ are defined by

$$\tilde{\boldsymbol{\tau}}^{\mathrm{s}} = 2\eta_{\mathrm{s}}\tilde{\boldsymbol{D}},\ \tilde{\boldsymbol{\tau}}^{\mathrm{p}} + \lambda\overset{\nabla}{\tilde{\boldsymbol{\tau}}}^{\mathrm{p}} = 2\eta_{\mathrm{p}}\tilde{\boldsymbol{D}}, \tag{3}$$

where λ is the fluid relaxation time and η_{s}, η_{p} the viscosity contribution from the solvent and the polymers, respectively. The symbol "∇" stands here for the upper-convected derivative which, for an arbitrary second-order tensor $\tilde{\boldsymbol{S}}$ with coordinates $\tilde{\boldsymbol{S}}_{ij}$ relative to a rectangular coordinate system, is

$$\overset{\nabla}{\tilde{\boldsymbol{S}}}_{ij} = \frac{\partial\tilde{\boldsymbol{S}}_{ij}}{\partial\tilde{t}} + \tilde{\boldsymbol{v}}_k\frac{\partial\tilde{\boldsymbol{S}}_{ij}}{\partial\tilde{x}_k} - \frac{\partial\tilde{\boldsymbol{v}}_i}{\partial\tilde{x}_k}\tilde{\boldsymbol{S}}_{kj} - \tilde{\boldsymbol{S}}_{ik}\frac{\partial\tilde{\boldsymbol{v}}_j}{\partial\tilde{x}_k}. \tag{4}$$

The $\tilde{\boldsymbol{D}}$ in Eq.(3) called rate of deformation tensor is the symmetric part of the velocity gradient. The components of $\tilde{\boldsymbol{D}}$ relative to a rectangular coordinate system are

$$\tilde{D}_{ij} = \frac{1}{2}\left(\frac{\partial\tilde{v}_i}{\partial\tilde{x}_j} + \frac{\partial\tilde{v}_j}{\partial\tilde{x}_i}\right). \tag{5}$$

If η_{p}=0, the Oldroyd-B equation reduces to the upper converted Maxwell constitutive equation, if λ=0, it further reduces to the Newtonian constitutive equation.

The non-dimensional quantities are introduced as follows:

$$(x,y,s) = \frac{(\tilde{x},\tilde{y},\tilde{s})}{a},\ (u,v,w) = \frac{(\tilde{u},\tilde{v},\tilde{w})}{W_{\mathrm{o}}},\ p = \frac{a\tilde{p}}{\eta W_{\mathrm{o}}},$$

$$\boldsymbol{\tau}^{\mathrm{s}} = \frac{a}{\eta W_{\mathrm{o}}}\tilde{\boldsymbol{\tau}}^{\mathrm{s}},\ \boldsymbol{\tau}^{\mathrm{p}} = \frac{a}{\eta W_{\mathrm{o}}}\tilde{\boldsymbol{\tau}}^{\mathrm{p}},\quad \kappa = \frac{a}{R},$$

$$W_o=\frac{a^2}{4\eta}\left(-\frac{\partial\tilde{p}}{\partial\tilde{s}}\right)=\frac{Ga^2}{4\eta},\ Re=\frac{\rho W_o a}{\eta},\ We=\frac{\lambda W_o}{a}, \quad (6)$$

where W_o is a characteristic velocity of the flow and η is the sum of η_p and η_s. p is the non-dimensional pressure. It is assumed that the Oldroyd-B fluid flow is fully developed and incompressible. For fully developed flows, the velocity field is independent of $\tilde{s}$, consequently the axial component of the pressure gradient $\partial\tilde{p}/\partial\tilde{s}$ is a constant denoted as $-G$. Using the definition of W_o and p, the negative of the axial component of the non-dimensional pressure gradient, $\partial p/\partial s$, takes the value of 4. κ is the non-dimensional curvature ratio; ρ is the density of the fluid; Re is the Reynolds number; We is the Weissenberg number. For fully developed impressible flow of Oldroyd-B fluid in curved pipes, the non-dimensional continuity equation, the non-dimensional momentum equation and the non-dimensional constitutive equation are given as:

$$Re\left[u\frac{\partial u}{\partial x}+v\frac{\partial v}{\partial y}-\frac{\kappa}{M}w^2\right]=-\frac{\partial p}{\partial x}+\left[\frac{\partial\tau_{xx}}{\partial x}+\frac{\partial\tau_{xy}}{\partial y}+\frac{\kappa}{M}(\tau_{xx}-\tau_{ss})\right], \quad (7)$$

$$Re\left[u\frac{\partial v}{\partial x}+v\frac{\partial v}{\partial y}\right]=-\frac{\partial p}{\partial y}+\left[\frac{\partial\tau_{xy}}{\partial x}+\frac{\partial\tau_{yy}}{\partial y}+\frac{\kappa}{M}\tau_{xy}\right], \quad (8)$$

$$Re\left[u\frac{\partial w}{\partial x}+v\frac{\partial w}{\partial y}+\frac{\kappa}{M}uw\right]=-\frac{1}{M}\frac{\partial p}{\partial s}+\left[\frac{\partial\tau_{xs}}{\partial x}+\frac{\partial\tau_{ys}}{\partial y}+\frac{2\kappa}{M}\tau_{xs}\right], \quad (9)$$

$$\frac{\partial u}{\partial x}+\frac{\partial v}{\partial y}+\frac{\kappa}{M}u=0, \quad (10)$$

$$\tau_{xx}^{p}+We\left[u\frac{\partial\tau_{xx}^{p}}{\partial x}+v\frac{\partial\tau_{xx}^{p}}{\partial y}-2\tau_{xx}^{p}\frac{\partial u}{\partial x}-2\tau_{xy}^{p}\frac{\partial u}{\partial y}\right]=2\frac{\eta_p}{\eta}\frac{\partial u}{\partial x}, \quad (11)$$

$$\tau_{xy}^{p}+We\left[u\frac{\partial\tau_{xy}^{p}}{\partial x}+v\frac{\partial\tau_{xy}^{p}}{\partial y}-\tau_{xy}^{p}\left(\frac{\partial u}{\partial x}+\frac{\partial v}{\partial y}\right)-\tau_{xx}^{p}\frac{\partial v}{\partial y}-\tau_{yy}^{p}\frac{\partial u}{\partial y}\right]=\frac{\eta_p}{\eta}\left(\frac{\partial u}{\partial y}+\frac{\partial v}{\partial x}\right), \quad (12)$$

$$\tau_{xs}^{p}+We\left[u\frac{\partial\tau_{xs}^{p}}{\partial x}+v\frac{\partial\tau_{xs}^{p}}{\partial y}-\tau_{xs}^{p}\frac{\partial u}{\partial x}-\tau_{xx}^{p}\frac{\partial w}{\partial y}-\tau_{ys}^{p}\frac{\partial u}{\partial x}-\tau_{xy}^{p}\frac{\partial w}{\partial y}+\frac{\kappa}{M}(\tau_{xx}^{p}w-\tau_{xs}^{p}u)\right]=\frac{\eta_p}{\eta}\left(\frac{\partial w}{\partial x}-\frac{\kappa}{M}w\right), \quad (13)$$

$$\tau_{yy}^{p}+We\left[u\frac{\partial\tau_{yy}^{p}}{\partial x}+v\frac{\partial\tau_{yy}^{p}}{\partial y}-2\tau_{xy}^{p}\frac{\partial v}{\partial x}-2\tau_{yy}^{p}\frac{\partial v}{\partial y}\right]=2\frac{\eta_p}{\eta}\frac{\partial v}{\partial y}, \quad (14)$$

$$\tau_{ys}^{p}+We\left[u\frac{\partial\tau_{ys}^{p}}{\partial x}+v\frac{\partial\tau_{ys}^{p}}{\partial y}-\tau_{xs}^{p}\frac{\partial v}{\partial x}-\tau_{xy}^{p}\frac{\partial w}{\partial x}-\tau_{ys}^{p}\frac{\partial v}{\partial y}-\tau_{yy}^{p}\frac{\partial w}{\partial y}+\frac{\kappa}{M}(\tau_{xy}^{p}w-\tau_{ys}^{p}u)\right]=\frac{\eta_p}{\eta}\frac{\partial w}{\partial y}, \quad (15)$$

$$\tau_{ss}^{p}+We\left[u\frac{\partial\tau_{ss}^{p}}{\partial x}+v\frac{\partial\tau_{ss}^{p}}{\partial y}-2\tau_{xs}^{p}\frac{\partial w}{\partial x}-2\tau_{ys}^{p}\frac{\partial w}{\partial y}+\frac{\kappa}{M}(2\tau_{xs}^{p}w-\tau_{ss}^{p}u)\right]=2\frac{\eta_p}{\eta}\frac{\kappa}{M}u, \quad (16)$$

$$\tau_{xx}^{s}=2\frac{\eta_s}{\eta}\frac{\partial u}{\partial x}, \quad (17)$$

$$\tau_{xy}^{s}=\frac{\eta_s}{\eta}\left(\frac{\partial u}{\partial y}+\frac{\partial v}{\partial x}\right), \quad (18)$$

$$\tau_{xs}^{s}=\frac{\eta_s}{\eta}\left(\frac{\partial w}{\partial x}-\frac{\kappa}{M}w\right), \quad (19)$$

$$\tau_{yy}^{s}=2\frac{\eta_s}{\eta}\frac{\partial v}{\partial y}, \quad (20)$$

$$\tau_{ys}^{s}=\frac{\eta_s}{\eta}\frac{\partial w}{\partial y}, \quad (21)$$

$$\tau_{ss}^{s}=2\frac{\eta_s}{\eta}\frac{\kappa}{M}u, \quad (22)$$

where $M=1+\kappa x$. (23)

The stream function ψ satisfying the continuity function equation, is defined as

$$u=\frac{1}{M}\frac{\partial\psi}{\partial y}=\frac{1}{M}\psi_y,\ v=-\frac{1}{M}\frac{\partial\psi}{\partial x}=-\frac{1}{M}\psi_x. \quad (24)$$

After substituting Eq.(24) into Eq.(9), the equations are as

$$\frac{Re}{M}\left[\psi_y\frac{\partial w}{\partial x}+\psi_x\frac{\partial w}{\partial y}+\frac{\kappa}{M}\psi_y w\right]=-\frac{\partial p}{\partial s}+\left[\frac{\partial \tau_{xs}}{\partial x}+\frac{\partial \tau_{ys}}{\partial y}+\frac{2\kappa}{M}\tau_{xs}\right]. \tag{25}$$

The stream function for Eq.(7) and Eq.(8) is obtained by substituting Eq.(24) in the two equations, differentiating Eq.(7) with respect to y and adding the result to the negative of the derivative with respect to x of Eq.(8). The result is

$$\begin{aligned}\frac{Re}{M^2}&\left[2\frac{\partial^2\psi}{\partial y^2}\frac{\partial^2\psi}{\partial x\partial y}+\frac{\partial^3\psi}{\partial y^2\partial x}\frac{\partial\psi}{\partial y}+\frac{\partial^3\psi}{\partial y^3}\frac{\partial\psi}{\partial x}\right.\\&\left.-\left(2\frac{\partial^2\psi}{\partial x^2}\frac{\partial^2\psi}{\partial x\partial y}+\frac{\partial^3\psi}{\partial x^2\partial y}\frac{\partial\psi}{\partial x}+\frac{\partial^3\psi}{\partial x^3}\frac{\partial\psi}{\partial y}\right)\right]\\&=-\frac{\partial^2\tau_{xy}}{\partial x^2}+\frac{\partial^2\tau_{xy}}{\partial y^2}+\frac{\partial^2\tau_{xx}}{\partial x\partial y}-\frac{\partial^2\tau_{yy}}{\partial x\partial y}\\&\quad+\frac{k}{M}\left(\frac{\partial\tau_{xx}}{\partial y}-\frac{\partial\tau_{xy}}{\partial x}-\frac{\partial\tau_{ss}}{\partial y}\right).\end{aligned} \tag{26}$$

The boundary conditions are:

$$w|_\Gamma=0,\ \psi|_\Gamma=u|_\Gamma=v|_\Gamma,\ \partial\psi/\partial n=0 \tag{27}$$

where Γ and n are the wall boundary of the pipes and the independent variable along the direction of the inner normal of the wall boundary, respectively.

GALERKIN METHOD

The Galerkin method is adopted to investigate flow through curved pipes with circular cross-section.

According to Xue (2002)'s work, first, the base function series $\{\psi_i\}$, $\{w_j\}$, $\{\tau^{\mathrm{p}}_{xx\,j}\}$, $\{\tau^{\mathrm{p}}_{xy\,i}\}$, $\{\tau^{\mathrm{p}}_{xs\,j}\}$, $\{\tau^{\mathrm{p}}_{yy\,j}\}$, $\{\tau^{\mathrm{p}}_{ys\,i}\}$ and $\{\tau^{p}_{ss\,j}\}$ (i, j=1, 2, …) are chosen, the variables are expressed as

$$\begin{aligned}&\psi=\sum_{i=0}^{m_1}a_i\psi_i,\ w=\sum_{j=0}^{m_2}b_j w_j,\ \tau^{\mathrm{p}}_{xx}=\sum_{j=0}^{m_2}c_j\tau^{\mathrm{p}}_{xx\,j}\\&\tau^{\mathrm{p}}_{xy}=\sum_{i=0}^{m_1}d_i\tau^{\mathrm{p}}_{xy\,i},\ \tau^{\mathrm{p}}_{xs}=\sum_{j=0}^{m_2}e_j\tau^{\mathrm{p}}_{xs\,j},\ \tau^{\mathrm{p}}_{yy}=\sum_{j=0}^{m_2}f_j\tau^{\mathrm{p}}_{yy\,j}\\&\tau^{\mathrm{p}}_{ys}=\sum_{i=0}^{m_1}g_i\tau^{\mathrm{p}}_{ys\,i},\ \tau^{\mathrm{p}}_{ss}=\sum_{j=0}^{m_2}h_j\tau^{\mathrm{p}}_{ss\,j}.\end{aligned} \tag{28}$$

where m_1 and m_2 denote the number of the terms of series $\{\psi_i\}$ and $\{w_j\}$. In curved pipes variables ψ, for τ^{p}_{xy} and τ^{p}_{ys} are antisymmetric and w, τ^{p}_{xx}, τ^{p}_{yy} and τ^{p}_{ss} symmetric, the numbers of the terms of series $\{\tau^{\mathrm{p}}_{xy\,i}\}$ and $\{\tau^{\mathrm{p}}_{ys\,i}\}$ are the same as those of series $\{\psi_i\}$. And so are those in the case of symmetric variables.

Considering the boundary condition, the ψ_i and the w_j are simply given as follows:

$$\psi_i=[1-(x^2+y^2)]^2\alpha_i,\ w_j=[1-(x^2+y^2)]\beta_j. \tag{29}$$

The components of $\boldsymbol{\tau}^{\mathrm{p}}$ are as follows:

$$\begin{aligned}&\tau^{\mathrm{p}}_{xx\,j}=\beta_j,\ \tau^{\mathrm{p}}_{xy\,i}=\alpha_i,\ \tau^{\mathrm{p}}_{xs\,i}=\beta_i,\\&\tau^{\mathrm{p}}_{yy\,j}=\beta_j,\ \tau^{\mathrm{p}}_{ys\,i}=\alpha_i,\ \tau^{\mathrm{p}}_{ss\,j}=\beta_j.\end{aligned} \tag{30}$$

Series $\{\alpha_i\}$ and $\{\beta_j\}$ must be linearly independent. The forms of $\{\alpha_i\}$ and $\{\beta_j\}$ in the present work are as follows:

$$\{\alpha_i\}=\{y,xy,x^2y,y^3,x^3y,xy^3,x^4y,x^2y^3,y^5,x^5y,x^3y^3,xy^5\}, \tag{31}$$

$$\{\beta_j\}=\{1,x,x^2,y^2,x^3,xy^2,x^4,x^2y^2,y^4,x^5,x^3y^2,xy^4,x^6,x^4y^2,x^2y^4,y^6\} \tag{32}$$

Second, substituting Eqs.(29) and (30) into Eqs.(11)~(22), (25) and (26) and integrating them by Galerkin criterion, with the aid of computer symbolic manipulation technique, a set of non-linear equations on a_i to h_j can be obtained. The Newton-Raphson method is adopted to solve the resulted non-linear equations. With the coefficients a_i to h_j being obtained, it is easy to obtain both the whole flow structure and the distribution of extra stresses. Similar to other numerical methods, the Galerkin method also considers accuracy. The global accuracy of the method is determined by the number of base function terms. In Fig.2, we present the contours of axial velocity for Re=25, η_{p}/η=0.2, We=5, κ=0.1 in two different sets of base functions. In one set the maximum powers of terms for stream function, axial velocity and extra stresses are 6 while in the other set the powers are 7. The two contours are almost the same. Taking both the accuracy and CPU time into consideration, the former set of base functions are chosen for the rest of the computations.

Comparisons with the available results in Fig.3

showed that the Galerkin results of the present work and the perturbation results of Robertson's work confirm each other very well.

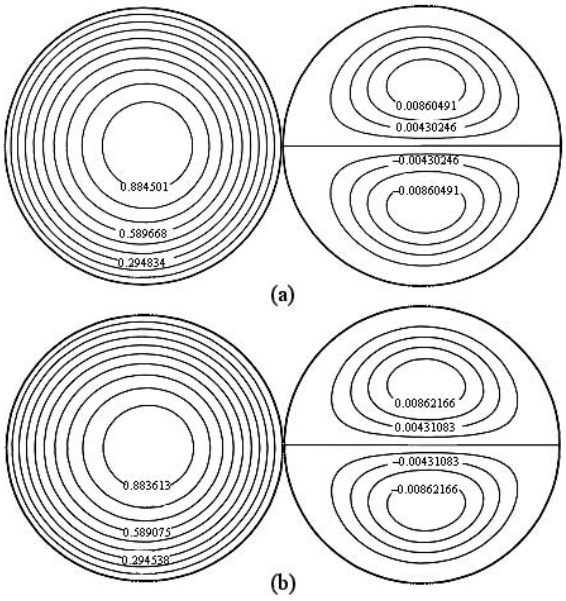

Fig.2 Comparisons of the Oldroyd-B fluid flow in curved pipe of w (left) and ψ (right). (Re=25, η_p/η=0.2, We=5, κ=0.1). (a) 6 powers solution; (b) 7 powers solution

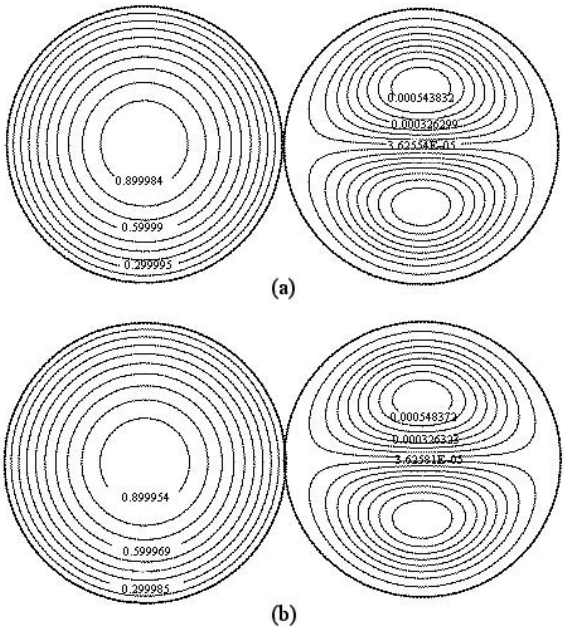

Fig.3 Comparisons of the Oldroyd-B fluid flow in curved pipe of w (left) and ψ (right). (Re=10, η_p/η=0.2, We=5, κ=0.01). (a) Present work; (b) Robertson's work

RESULTS AND DISCUSSION

Because of the small parameters limit of perturbation technique, the curvature ratio, the Reynolds number and the Weissenberg number of the perturbation solutions reported are limited to less than 0.1, 25 and 5, respectively. However, in the present work such parameters can be much larger by using Galerkin method.

The axial flow of Oldroyd-B fluid in curved pipes is showed in Fig.4 and Fig.5. One of the distinctions between Newtonian and Oldroyd-B fluids is in the degree of inward or outward shift of the maximum in axial velocity. It can be observed in Fig.5 that for small Reynolds number, the maximum in axial velocity is shifted toward the inner bend of the pipe. The inward shift decreases and becomes an outward shift gradually as Re or We is increased. Fig.4 is the example of outward shift (Re=25, η_p/η=0.2, We=8, and κ=0.1). However, for the case of large values of Re, the maximum in axial velocity is shifted outward for values of We beyond a critical value. The critical values of We decrease with increasing Re. The non-linear interaction of inertia and elasticity results in a greater shift toward the outer bend in the case of small values of Re. For large value of Re such interaction results in a smaller outward shift than in the non-elastic case as the We becomes bigger enough such as shown in the curve of Re=50 in Fig.5.

In curved pipes, centripetal acceleration and fluid elasticity cause secondary flow characterized by a pair of counter-rotating vortices. Fig.6 is a represen-

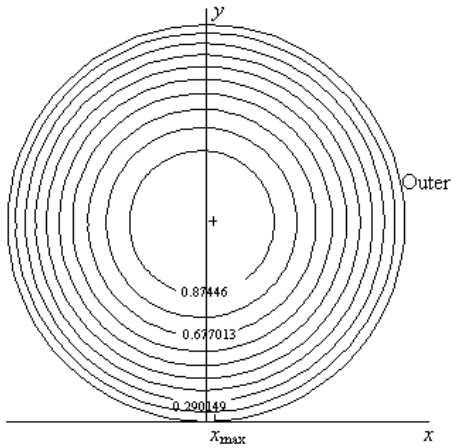

Fig.4 Contours of axial velocity for Re=25, η_p/η=0.2, We=8, and κ=0.1

tative one of the contours of stream function in curved pipes. To compare Fig.7 with the Robertson and Muller (1996)'s analogous result, it is obvious that for small value of Reynolds number, the outward shift of maximum increases monotonously as Weissenberg number is increased, but for large value of *Re*, the monotonicity is broken. Together with the result of axial flow discussed above, the vanishing of the monotonicities indicates that the combined effect of inertia and elasticity is much weaker than the independent effect of inertia or elasticity as Reynolds number and Weissenberg number are both large enough, which is the result of the complex non-linear interaction of inertia and elasticity with large parameters.

The volume flux, written with respect to the non-dimensional variables introduced in Eq.(6), is

$$Q = W_o a^2 \int_{-1}^{1} \int_{-\sqrt{1-x^2}}^{\sqrt{1-x^2}} w \mathrm{d}y \mathrm{d}x . \quad (33)$$

The volume flux in a curved pipe is denoted by Q_c, and that in a straight pipe of the same flow parameter by Q_s. In the present work, Q_s equals $\pi W_o a^2/2$. The volume flux ratio is defined as

$$\frac{Q_c}{Q_s} = \frac{W_o a^2 \int_{-1}^{1} \int_{-\sqrt{1-x^2}}^{\sqrt{1-x^2}} w \mathrm{d}y \mathrm{d}x}{\pi W_o a^2 / 2} = \frac{\int_{-1}^{1} \int_{-\sqrt{1-x^2}}^{\sqrt{1-x^2}} w \mathrm{d}y \mathrm{d}x}{\pi / 2} . \quad (34)$$

The flow resistance (the friction factor) is generally expressed in terms of the reciprocal of the volume flux ratio

$$f_s/f_c = Q_c/Q_s. \quad (35)$$

Fig.8 indicates that for the case of creeping flow, the effect of increasing Weissenberg number strengthens flow resistance, which is just the opposite to the effect for the case of large value of Reynolds number.

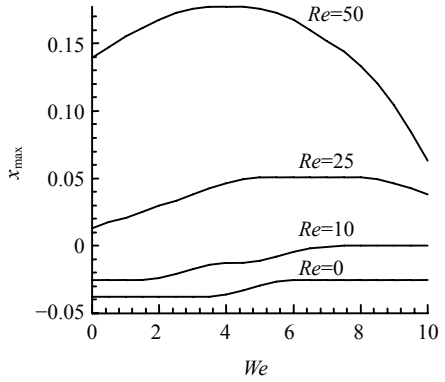

Fig.5 Location of maximum in axial velocity as a function of *We* for η_p/η=0.2 and κ=0.1

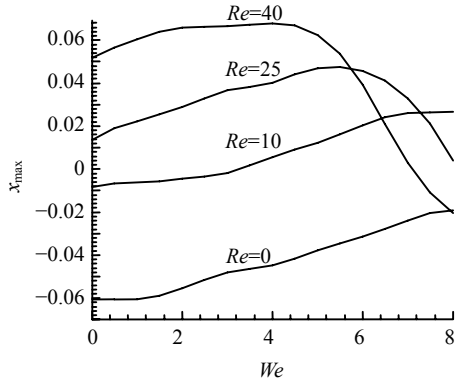

Fig.7 Location of maximum in stream function as a function of *We* for η_p/η=0.2 and κ=0.2

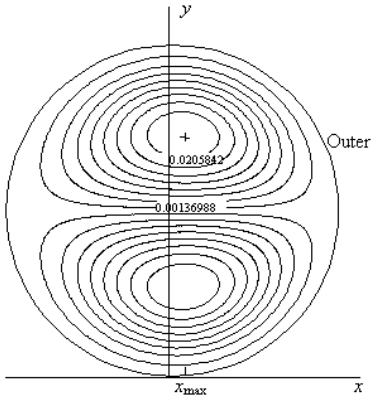

Fig.6 Contours of stream function for *Re*=40, η_p/η=0.2, *We*=5 and κ=0.2

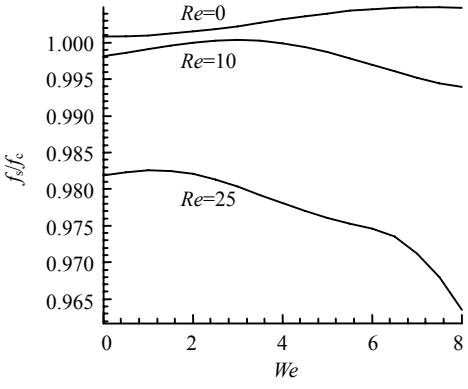

Fig.8 Location of friction factor as a function of *We* for η_p/η=0.2 and κ=0.2

The axial normal stress, τ_{ss}, is another distinction between Newtonian fluids and Oldroyd-B fluids. Through analysis of the constitutive equations, it is easy to find that there is no relationship between the axial normal stress and the axial flow velocity in Newtonian case, while in Oldroyd-B case such relationship has been established, so the value of τ_{ss} in Oldroyd-B case is much larger than in Newtonian case.

Fig.9 shows the variation of contours of axial normal stress with *We* in creeping flow, which indicates the effects of elasticity on the axial normal stress. For creeping flow, similar with the distribution of axial flow velocity, the maximum in axial normal stress is near the inner bend of the pipe. With increasing elasticity, the distribution of axial normal stress becomes more and more even. Meanwhile, the maximum in axial normal stress concentrates near the center of the inner bend of the pipe. The location of the minimum of τ_{ss} extends to the outer bend of the pipe with increasing Weissenberg number. Such variation of axial normal stress is just the result of the variation of axial flow velocity affected by the elasticity.

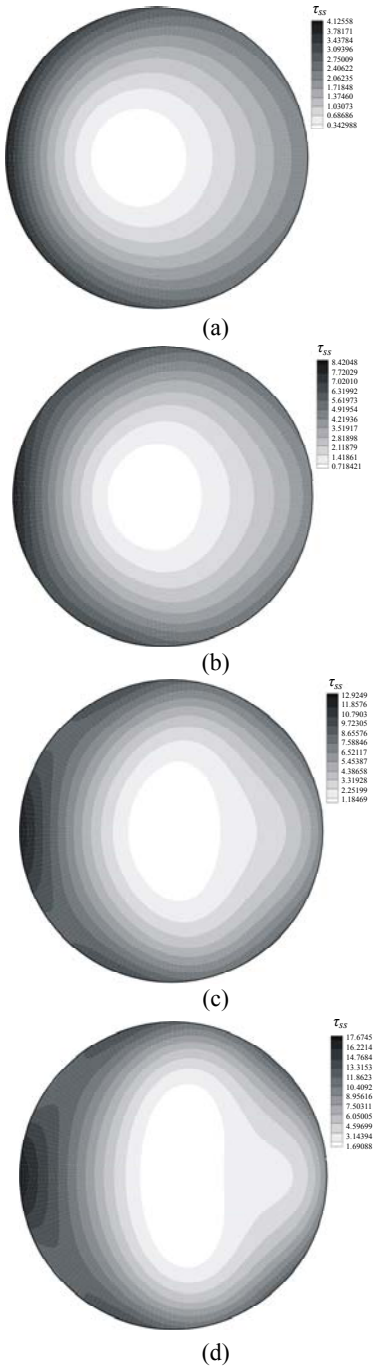

Fig.9 Contours of axial normal stress for *Re*=0, η_p/η=0.2 and κ=0.2. (a) *We*=2; (b) *We*=4; (c) *We*=6; (d) *We*=8

CONCLUSION

The flow of Oldroyd-B fluid in curved pipes was investigated by Galerkin method. The scales of the curvature ratio, the Reynolds number and the Weissenberg number are widely extended by using Galerkin method. The coupled effect of inertia and elasticity on Oldroyd-B fluid flow in curved pipes was examined in detail. The major conclusions drawn are as follows:

For small value of Reynolds number, the effect of increasing Weissenberg number gradually shifts the maximum stream function and maximum axial velocity toward the outer bend of the pipe. However, for the case of large Reynolds number, both the monotonicities are broken because of the combined non-linearity of large values of Reynolds number and Weissenberg number.

The distribution of τ_{ss} is also dependent on the Weissenberg number. Through the study of creeping flow of Oldroyd-B fluid, the independent effect of the Weissenberg number on the distribution of τ_{ss} can be discovered. The maximum value in τ_{ss} concentrates near the center of the inner bend of the pipe with increasing Weissenberg number, while the distribution of the minimum τ_{ss} extends to the outer bend of the pipe.

References

Bolinder, C.J., 1996. Curvilinear coordinates and physical components: an application to the problem of viscous flow and heat transfer in smoothly curved ducts. *J. Appl. Mech.*, **63**:985-989.

Bowen, P.J., Davies, A.R., Walters, K., 1991. On viscoelastic effects in swirling flows. *J. Non-Newtonian Fluid Mech.*, **38**(2-3):113-126. [doi:10.1016/0377-0257(91)83001-K]

Chen, H.J., Zhang, B.Z., Su, X.Y., 2003. Low frequency oscillatory flow in a rotating curved pipe. *J. Zhejiang University SCIENCE*, **4**(4):407-414.

Clegg, D.B., Power, G., 1963. Flow of a Bingham fluid in a slightly curved tube. *Appl. Sci. Res.*, **12**:199-212.

Das, B., 1992. Flow of a Bingham fluid in a slightly curved tube. *Int. J. Engng. Sci.*, **30**(9):1193-1207. [doi:10.1016/0020-7225(92)90067-Q]

Dean, R.W., 1927. Note on the motion of fluid in a curved pipe. *Phil. Mag.*, **7**(4):208-223.

Dean, R.W., 1928. The stream-line motion of fluid in a curved pipe. *Phil. Mag.*, **7**(5):673-695.

Fan, Y.R., Tanner, R.I., Phan-Thien, N., 2001. Fully developed viscous and viscoelastic flows in curved pipes. *J. Fluid Mech.*, **440**:327-357. [doi:10.1017/S0022112001004785]

Ito, H., 1969. Laminar flow in curved pipes. *Z. Angew. Math. Mech*., **49**:653-662.

Jitchote, W., Robertson, A.M., 2000. Flow of second order fluids in curved pipes. *J. Non-Newtonian Fluid Mech.*, **90**(1):91-116. [doi:10.1016/S0377-0257(99)00070-1]

Jones, C.R., 1960. Flow of a non-Newtonian liquid in a curved pipe. *Quart. J. Mech. Appl. Math.*, **13**:428-443.

Nandakumar, K., Masliyah, H.J., 1982. Bifurcation in steady laminar flow through curved pipes. *J. Fluid. Mech.*, **119**:475-490. [doi:10.1017/S002211208200144X]

Robertson, A.M., Muller, S.J., 1996. Flow of Oldroyd-B fluids in curved pipes of circular and annular cross-section. *J. Non-linear Mech.*, **31**(1):1-20. [doi:10.1016/0020-7462(95)00040-2]

Sharma, H.G., Prakash, A., 1977. Flow of second-order fluid in a curved pipe. *Indian J. Pure Appl. Math.*, **8**:546-557.

Soh, W.Y., Berger, S.A., 1987. Fully developed flow in a curved pipe of arbitrary curvature ratio. *International Journal for Numerical Methods in Fluids*, **7**(7):733-755. [doi:10.1002/fld.1650070705]

Thomas, A.H., Walters, K., 1963. On the flow of an elastico-viscous liquid in a curved pipe under a pressure gradient. *J. Fluid Mech.*, **16**(2):228-242. [doi:10.1017/S0022112063000719]

Topakoglu, C.H., 1967. Steady laminar flows of an incompressible viscous fluid in curved pipes. *J. Math. Mech.*, **16**:1321-1337.

Xue, L., 2002. Study on laminar flow in helical circular pipes with Galerkin method. *Computers & Fluids*, **31**(1):113-129. [doi:10.1016/S0045-7930(00)00013-X]

Zhang, J.S., Zhang, B.Z., 2003. Dean equations extended to rotating helical pipe flow. *J. Engrg. Mech.*, **129**(7):823-829. [doi:10.1061/(ASCE)0733-9399(2003)129:7(823)]

Zhang, J.S., Zhang, B.Z., Chen, H.J., 2000. Flow in helical annular pipe. *J. Engrg. Mech.*, **126**(10):1040-1047. [doi:10.1061/(ASCE)0733-9399(2000)126:10(1040)]